

EXPERIMENTAL INVESTIGATION OF POLYURETHANE-COATED HPFRC PANELS UNDER DIRECT CONTACT BLAST

ALŽBĚTA MĚRKOVÁ^{a,*}, PŘEMYSL KHEML^a, ALEXANDRE PERROT^b,
PETR HÁLA^a

^a Czech Technical University in Prague, Faculty of Civil Engineering, Experimental Centre, Thákurova 7, 166 29 Prague, Czech Republic

^b SYNPO, akciová společnost, S. K. Neumanna 1316, 532 07 Pardubice, Czech Republic

* corresponding author: alzbeta.merkova@fsv.cvut.cz

ABSTRACT. High-performance fibre-reinforced concrete (HPFRC) exhibits exceptional resistance to dynamic loading, making it a promising material for structures exposed to blast or impact events. However, when used to produce thin panels, it can experience scabbing under extreme loads. To address this and enhance the blast resistance, this study explores the application of a polyurethane (PU) coating to the HPFRC panels. Coated and uncoated panels undergo direct contact blast testing and various factors, such as crater area, rear fragment formation, cracking, and residual flexural strength, are analysed. Our study indicates that applying a PU coating to the panels could effectively prevent scabbing and mitigate the risk of complete perforation, while it appears that it results in the panel absorbing more energy during blast, leading to increased damage and a subsequent decrease in residual flexural strength compared to bare panels.

KEYWORDS: High-performance fibre-reinforced concrete, elastomeric coating, thin panel, direct contact explosion, experimental study.

1. INTRODUCTION

The emphasis on the development of protective structures capable of withstanding extreme loading has become a major concern within the field of structural engineering. In response to this imperative, a new modular blast and ballistic system was introduced in [1]. This system features high-performance fibre-reinforced concrete panels of specific shapes, designed to interlock and create protective structures of various shapes and purposes. In addition, assembly can be quickly performed manually without the need for heavy machinery, and since the structure is self-supporting, no supports, foundations, or anchoring are necessary. Other benefits of the system include attributes such as lightweight construction, versatility, flexibility, and mobility. Its applicability is primarily as mobile city barriers, special checkpoints, fortified posts, barricades, protective structures in ballistic centres, and other.

Several research groups have conducted experimental studies to examine the behaviour and response of HPFRC panels under various loading conditions. Mára et al. [2] investigated the resistance of both individual panels and assembled wall configurations to static, ballistic, and blast loading. In their blast experiments on the HPFRC panels, they analysed the effects of a 75 g TNT charge at stand-off distances ranging from 0 to 1 000 mm. Results indicated that at a stand-off distance of 750 mm or more, no visible damage occurred, while distances between 250 mm and 500 mm caused frontal erosion without complete

perforation. Direct contact with the 75 g TNT charge resulted in local complete perforation of the panel. Subsequent experiments maintained a constant stand-off distance of 1 000 mm while varying the TNT charge from 75 g to 2 000 g. Findings showed that up to 300 g TNT, no visible damage occurred, while between 400 g and 800 g, frontal erosion without perforation or scabbing occurred. Charges ranging from 1 200 g to 2 000 g led to global failure of the panel with no residual capacity. Overall, the results clearly demonstrate that damage increases with charge weight at a constant stand-off distance. Similarly, at a constant charge weight, damage increases with smaller stand-off distances, with the most critical scenario being direct contact between the charge and the panel.

Our study builds upon the blast findings of Mára et al. [2], where we specifically focus on identifying the setup that exerts the most significant impact on the sample. Their experiments clearly demonstrated that a complete perforation of the HPFRC panel occurred only when the 75 g TNT charge was placed in direct contact with it. Thus, we aim to replicate this setup while introducing a protective coating to prevent panel perforation.

HPFRC panels with protective coatings, using polyurethane (PU) to enhance the resistance against ballistic loading, were investigated in [3, 4]. They concluded that polyurethane-coated HPFRC panels show case significantly higher ballistic resistance compared to uncoated HPFRC panels. Notably, the efficacy of the PU coating in bolstering ballistic resistance across various materials, such as metal, concrete, and ceram-

ics, has been explored by multiple research groups (e.g. [5–7]), with significant improvements observed. The potential of polyurethane and polyurea coatings to enhance resistance against other types of extreme loading such as blast has been investigated by various research groups as well. Tekalur et al. [8] conducted an experimental study to investigate the impact of blast on a woven composite material made of E-Glass vinyl ester, with the addition of polyurea in various configurations. The blast load was applied using a shock tube. They assessed the blast resistance using three main parameters: macroscopic visual damage examination, microscopic damage examination, and real-time deflection measurements. Their findings revealed that applying the PU layer to the load-receiving side enhanced the performance of the plate by 25%, while incorporating the PU layer in the middle of a sandwich structure resulted in an improvement of over 100% compared to the plain-woven composite. Further research [9–11] explored the effects of polyurea coating on steel plates subjected to impulsive loads, particularly examining the influence of the polyurea's position relative to the loading direction. Both numerical and experimental results indicate that applying polyurea to the back side of the steel plates can improve energy absorption and help mitigate failure. Conversely, placing polyurea on the load-receiving side can amplify the initial shock effect and promote failure. Additionally, an experimental study [12] examined the effects of polyurea-coated composite steel plates in various configurations under blast conditions, focusing on failure modes and energy dissipation mechanisms. The results demonstrate that the structural configuration significantly influences failure modes due to impedance mismatching between the steel and polyurea layers. Distinct energy dissipation mechanisms were observed for polyurea layers depending on their configurations and the intensity of the blast. The findings indicate that rear-side sprayed and sandwiched plates exhibit a superior air blast resistance compared to monolithic steel plates, while impact-side and both-sides sprayed plates show inferior air blast resistance compared to monolithic steel plates. According to Mohotti et al. [13], applying polyurea coating to the back side of steel plates can reduce their residual deformation by approximately 20% during a near-field blast. Recently, the ability of flexible materials, such as polyurethane foam and polyurea, to attenuate the impact of a weak shock wave has been demonstrated in [14]. Their findings indicate that positioning polyurea on the impact side of a layered structure consisting of polyurea and polyurethane foam can reduce the shock wave overpressure by up to 93.3% and the impulse attenuation capacity is superior to that of single-layer structures.

The thickness of the coating plays a crucial role in the dynamic response of structures. Findings by Si et al. [5] indicate that while impact-side coated structures consistently demonstrated a better ballis-

tic performance than uncoated ones, increasing the polyurea thickness from 2.2 mm to 3.3 mm resulted in a decrease in established indicators, such as perforation diameter, the confining pressure of ceramic tiles, and the strengthening effect at high strain rates. Amini et al. [10] found that increasing the polyurea thickness on the front face of steel plates exacerbated the initial shock effect on the steel layer, while simultaneously increasing the effective tangent modulus of the plate. These opposing effects suggest that, depending on the conditions, increased polyurea thickness may either improve or degrade the shock performance of the steel plate. In contrast, when polyurea was applied to the back face, its increased thickness consistently improved the overall performance of the plate. In their research, Mohotti et al. [13] numerically modelled steel plates with a polyurea coating on the back face, varying in thickness from 6 mm to 20 mm. Their results showed that increasing the polyurea thickness reduced the residual deformation of the plate, while simultaneously increasing its aerial density. These findings are consistent with those of LeBlanc et al. [15], who studied the effect of polyurea coating on the response of curved E-Glass/Vinyl ester composite panels subjected to underwater explosions.

While multiple studies have been conducted investigating the effect of PU coating on various materials (steel, aluminium, ceramic, concrete) subjected to extreme loading, apart from the ballistic tests conducted in [3, 4], to the best of our knowledge, there is no existing evidence of experiments testing the enhanced resistance of HPFRC panels with PU coatings against extreme loading. Therefore, our study represents the first endeavour to conduct blast tests on polyurethane-coated HPFRC panels, aiming to fill this gap in research.

2. MATERIALS AND METHODS

2.1. HIGH-PERFORMANCE FIBRE-REINFORCED CONCRETE

This study primarily aims to explore the impact of polyurethane coating on the blast resistance of high-performance fibre-reinforced concrete (HPFRC) panels, specifically the panels designed as part of the modular blast and ballistic protective system introduced in [1]. The panels used in the blast tests measured 1.5 m in length and 0.4 m in width, with a thickness of 0.04 m. Each panel weighed less than 55 kg and featured a rectangular shape, punctuated by four cutouts, two in each longer side, enabling interlocking within the modular system.

The HPFRC was acquired as a pre-mixed dry blend, meticulously produced through a closely monitored process within an industrial facility. The composition and proportions are presented in Table 1. The mixture design and development is detailed in [16, 17].

The dry blend is transferred into a vertical mixer to commence mixing. Approximately 90% of the

	Proportions by weight	kg m ⁻³
Cement 42.5 R	1	794
Silica fume (Microsilica)	0.1	79
Silica powder	0.25	198
Silica sands 0.1 to 1.2 mm	1.6	1 270
HRWR (Superplasticiser)	0.01	8
Anti-foaming agent	0.001	0.8
Water	0.3	235
Steel fibres	0.17	157

TABLE 1. Proportions of the HPFRC with 1.5 % fibre volume content.

Property	Value	Standard deviation
Compressive strength	90.33 MPa	8.7 MPa
Tensile strength	4.22 MPa	0.67 MPa
Bulk density	2 351 kg m ⁻³	17.3 kg m ⁻³

TABLE 2. Mechanical properties of HPFRC with 1.5 % fibre volume content.

Testing machine	Analysis	Temperature ramp.; temp. range	Frequency; max. deformation	Specimen dimensions
DHR-2	Torsion	3 °C min ⁻¹ ; -50–160 °C	1 Hz; 1 %	26 mm × 10 mm × 3 mm

TABLE 3. Polyurethane parameters.

final volume of water is gradually added to the mixture, and mixing continues for 5–7 minutes. Fibres are then added manually during mixing for the next 5–7 minutes to prevent clumping. Subsequently, the remaining water is added, and the blend is mixed for additional 5 minutes. The entire mixing process takes less than 20 minutes, after which the mixture is poured into steel moulds. Each mould is typically cast in two layers and to eliminate any air bubbles, the mould is thoroughly vibrated using a vibrating table after each layer of concrete.

The essential mechanical properties of the material, outlined in Table 2, were determined through strict testing procedures. Compressive strength measurements were conducted on cylindrical samples measuring 150 mm in diameter and 300 mm in height. The testing involved applying a monotonic load application at an average rate of 36 MPa min⁻¹. In total, four samples underwent testing. Direct tensile strength was determined using dog bone-shaped samples with a central segment of 200 mm in length and a reduced cross-sectional area of 50 mm × 100 mm, applying a deformation-controlled test procedure at a loading speed of 0.294 mm min⁻¹. In total, five samples underwent testing. Importantly, all samples were tested no earlier than 28 days after casting.

2.2. POLYURETHANE ELASTOMER

Polyurethane elastomer (PU-elastomer) was a neat two-component thermoset, consisting of a telechelic

polyol thinned with castor oil (part A) and cured with an aromatic isocyanate (part B). Several additives were included in the compound, such as a defoamer, zeolite paste, and an accelerator. Parts A and B were thoroughly homogenised with a spatula and directly poured onto a precleaned concrete surface measuring 400 mm × 400 mm. The thickness of the coated layer was 10 mm, similar to the study by Hála et al. [3], and the elastomer was cured at room temperature for seven days prior to testing. The reticulated elastomer had a density of 0.998 g cm⁻³ at 23 °C (according to [18], method A), a tear strength of 1.39 N mm⁻¹ (according to [19]), and a glass transition temperature (T_g) of -31 °C (onset of storage modulus G'), determined through dynamic mechanical analysis (DMA). The corresponding measurement parameters are detailed in Table 3.

The damping factor, $\tan \delta$, of the PU-elastomer was assessed at different operating temperatures commonly encountered in various regions of the globe (-30 °C, 25 °C, 80 °C), along with various pulsations (frequency sweeps). The aim was to evaluate the material's ability to absorb energy under different conditions, ranging from low to high operating temperatures and frequencies of deformation. The DMA curves from the experiments are detailed in Figure 1.

Tensile properties at different strain rates were determined according to [20] using an Adamel Lhomargy DY36 Testing machine. In addition, tensile properties were determined at different operating temperatures

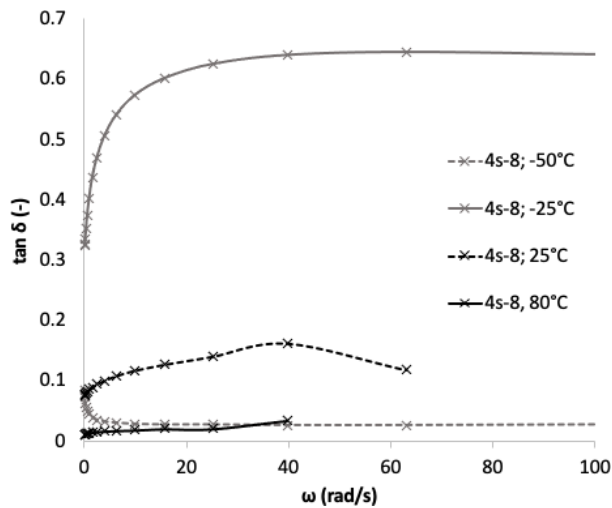


FIGURE 1. Damping factor of PU at different operating temperatures.

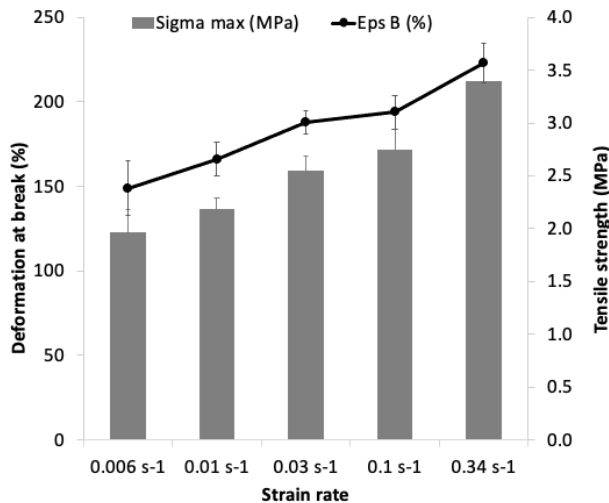


FIGURE 2. Tensile properties of PU at different strain rates.

(equally to DMA frequency sweep test), with a strain rate of 0.08 s^{-1} . The corresponding results are detailed in Figure 2.

The PU coating was applied to the centre of both sides of the HPFRC panel in a square shape with each side measuring 400 mm and a thickness of 10 mm. Given that the phenomenon under examination is localised, with the greatest loading occurring at the panel's centre, we opted not to coat the entire surface. Focusing the coating on the central area minimises material consumption, reduces costs, and lowers labour intensity. Notably, the damage observed during the blast tests was entirely confined to the polyurethane-coated area.

2.3. BLAST TEST

In contrast to Mára et al. [2], we opted for plastic explosive Semtex 1A in our experiments instead of TNT, primarily due to economic considerations, its availability, and versatility in being moulded into desired shapes directly on site. As we aimed to build upon

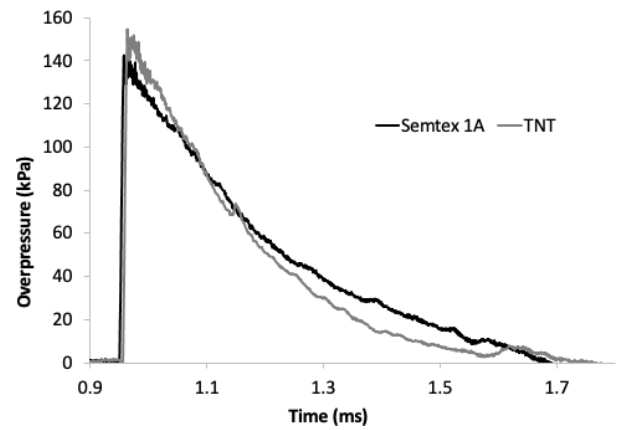


FIGURE 3. Comparison of 100 g TNT and Semtex 1A at 1 m stand-off distance.

prior research where a 75 g TNT charge in contact with HPFRC panels resulted in full penetration, we first compared the effectiveness of these two explosives to estimate the optimal Semtex 1A charge to yield similar outcomes. The explosive was suspended from a steel frame 1.5 m above the ground, and overpressure was measured using a pressure gauge, with the sensor positioned 1 m away from the charge. Consecutive detonations of 100 g charges of TNT and Semtex 1A were carried out to evaluate the effects of both explosives comparatively.

The findings indicate that both explosives produced comparable overpressure loading levels during a free-air blast, with a difference of approximately 10% observed in the maximum values, as illustrated in Figure 3. Based on the assumption that the characteristics and maximum values were sufficiently similar for the objectives of our study, we selected a 75 g Semtex 1A charge as the baseline for the blast tests, following up on the experiments conducted in [2].

The blast tests were conducted with the following setup: Each panel was positioned horizontally on two steel supports spaced 800 mm apart to ensure no contact with the ground. A metal detonator with a 75 g Semtex 1A charge was placed at the centre of the panel, in direct contact. Both coated and uncoated panels were tested to assess the effect of the PU coating on panel response. The charge was positioned in the centre directly on top of the panel. The setup is depicted in Figure 4.

A total of six samples were subjected to blast testing, with three coated on both sides with polyurethane and three left uncoated to assess the impact of the additional PU layers. Following the blast tests, we meticulously scanned the craters formed in the HPFRC panels using the DAVID SLS-2 scanning device.

2.4. QUASI-STATIC FOUR-POINT BENDING TEST

Following the blast tests, the panels were subjected to a quasi-static four-point bending test to determine their residual flexural strength. As a reference, three previously undamaged panels were subjected to the

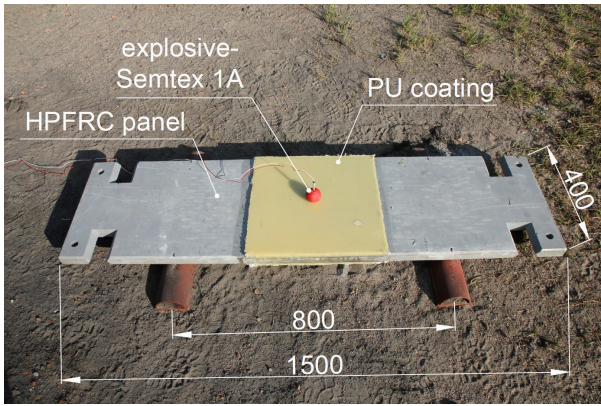


FIGURE 4. HPFRC panels blast test setup.

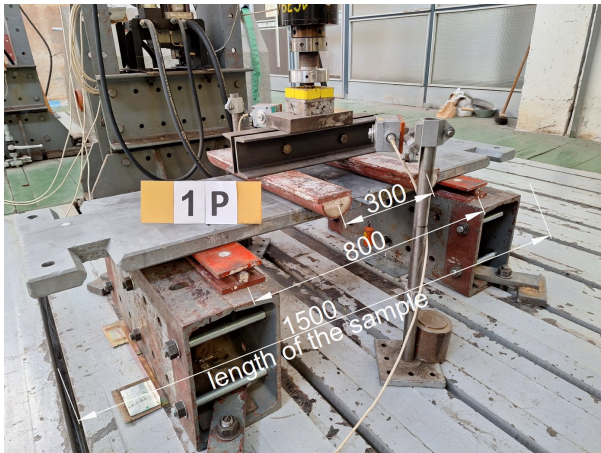


FIGURE 5. Configuration of quasi-static four-point bending test.

four-point bending test as well. This allowed us to evaluate the effect of the blast on the flexural strength of the panels as well as the effect of the additional PU coating. Each test was executed under displacement control at a predetermined rate of 1 mm min^{-1} . The panels were positioned horizontally atop two steel supports spaced 800 mm apart. The hydraulic jack exerted force on the panel's top surface through two centrally positioned points of contact, spaced 300 mm apart. The configuration of the four-point bending test is depicted in Figure 5. The test was terminated upon reaching a deflection of 16 mm in each sample. In all instances, the peak loading force was reached at this point and begun to decline.

3. RESULTS AND DISCUSSION

Our experimental objective was to determine the effect of polyurethane coating on the resistance of HPFRC panels to a direct contact explosion. To investigate this, we closely examined various factors including crater area, cracking, formation of rear fragments, as well as post-test bending strength.

Blast tests revealed that using 75 g Semtex 1A in direct contact with the sample resulted in a complete perforation of all bare HPFRC panels, as shown in

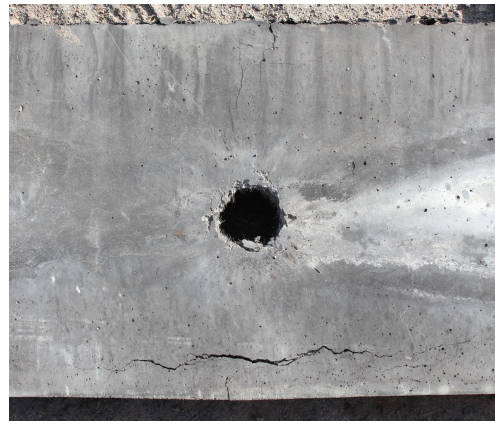


FIGURE 6. The effect of an explosion on an HPFRC panel without PU coating; impact side.



FIGURE 7. The effect of an explosion on an HPFRC panel without PU coating; rear side.

Figures 6 and 7. These findings are in accordance with the outcomes detailed in [2], where 75 g of TNT was used in direct contact with HPFRC panels. Furthermore, our results indicate that the addition of PU coating consistently prevented complete perforation in all instances, as depicted in Figures 8 and 9.

Our investigation reveals that the addition of PU coating significantly influenced the behaviour of the blast wave within the panel. When examining bare HPFRC panels, it appears that the blast wave traverses directly through and beyond the panel, leaving a distinct, single crater through the entire thickness of the panel, as illustrated in Figure 6. The resulting perforation is clean and there was no significant surface damage around the crater. In contrast, for PU-coated HPFRC panels, the blast wave appears to be partially reflected back upon reaching the interface between the PU layer and the front side of the HPFRC panel. It is very likely that this reflected wave causes lifting and subsequent fracture and detachment of the front PU coating from the HPFRC panel. Notably, in all cases, the front PU layer did not adhere to the panel but was detached during the blast test. Simultaneously, the blast wave passed through the panel and



FIGURE 8. The effect of an explosion on an HPFRC panel with PU coating on both sides; impact side.



FIGURE 9. The effect of an explosion on an HPFRC panel with PU coating on both sides; rear side.

was partially reflected when it reached the coated rear side. Figure 10 shows the impacted side of the panel. Analogous to the bare HPFRC panel, one primary crater forms. However, the crater is notably more fragmented and it is accompanied by increased damage to the edges and surrounding area. Spalling and multiple smaller craters also manifest on the front side of the panel. The deviation of the blast wave from a straight path through the panel suggests increased energy absorption by the panel, resulting in heightened frontal erosion, compared to bare panel. These observations resonate with the conclusions outlined in [11], where Amini et al. propose that front-side coating amplifies the blast energy transferred to the coated structure.

A detailed scan of the craters revealed differences in the crater areas on the front and back surfaces of the bare and coated panels, as detailed in Table 4. The results indicate that the average front surface crater area for coated samples is reduced by nearly 25%, while the average back surface crater area is almost 23% larger compared to bare panels. Notably, the average back surface crater is four times larger than the front crater for bare samples, whereas for PU-coated panels, it is nearly seven times larger, as shown in Figure 11. The enlargement of the back crater supports our hypothesis that the rear PU layer



FIGURE 10. Blast damage on the impacted side of an HPFRC panel with PU coating on both sides.

Sample	Front surface crater area [mm ²]	Back surface crater area [mm ²]
Bare	4 983.18	19 274.47
	5 719.53	23 868.74
	5 013.01	20 622.23
Coated	4 936.08	24 379.61
	4 253.87	26 817.22
	2 540.73	26 956.09

TABLE 4. The area of craters obtained by scanning.

diverts the blast wave from a straight path, leading to increased energy absorption by the panel.

The behaviour of a protective structure, particularly regarding the dispersion of flying rear concrete fragments, is paramount for the safety of individuals situated behind it. These flying fragments can cause damage to people and equipment. In the case of bare HPFRC panels, the blast induced fragmentation on the rear side of the panel, as illustrated in Figure 7. When testing PU-coated panels, the rear face of the HPFRC panel was also fragmented, but the PU coating prevented the fragments from flying off, resulting in bulging of the PU layer, as depicted in Figure 9. This observation indicates that applying PU coating to the back side of the panels significantly improves the protection of people and objects positioned behind the panels during the blast.

The blast loading induced cracking in all samples, manifesting distinct patterns depending on whether the HPFRC panels were bare or coated. In the case of bare HPFRC panels, the cracks that formed were few and exhibited a linear pattern, as depicted in Figures 6 and 7. The cracks appearing on the back surface are likely a result of tensile stress induced by the blast wave. Conversely, the coated panels exhibited more prominent cracking on the front surface, particularly beneath the front PU layer, as illustrated in Figure 10. The crack patterns on these coated panels displayed a distinct circular tendency, unlike the linear cracks

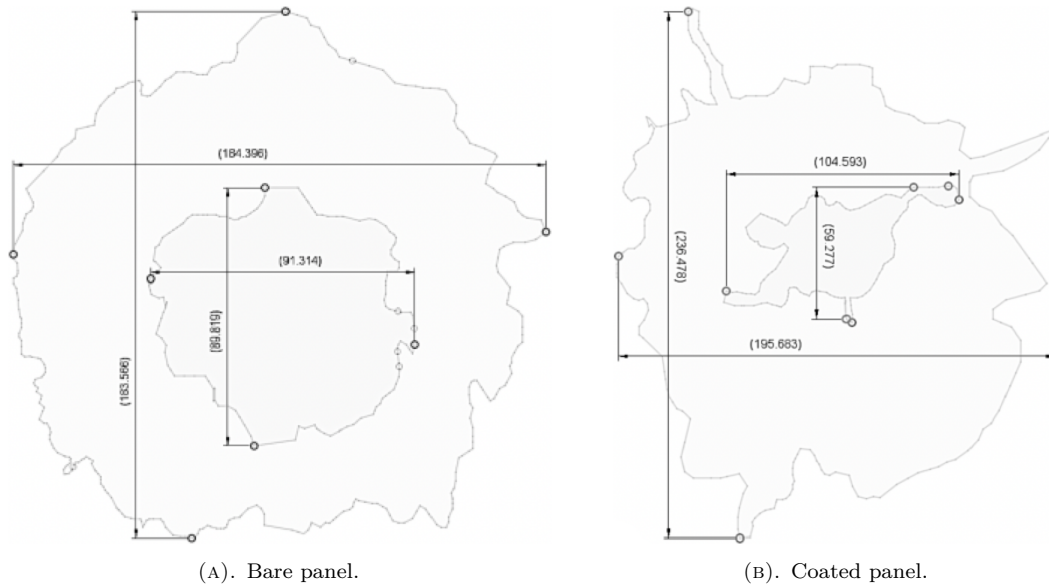


FIGURE 11. Comparison of the front and back surface crater for bare panel, coated panel.



FIGURE 12. Complete failure of a bare HPFRC panel due to blast; impact side.



FIGURE 13. Complete failure of a bare HPFRC panel due to blast; rear side.

seen in the bare panels. These circular cracks resemble the “hoop cracks” described in [12], where Hou et al. observed similar phenomena when subjecting steel plates, coated with polyurea on both sides, to air blast. Hou et al. [12] suggested that these hoop cracks result, among other factors, from deformation inconsistencies between the front PU layer and the underlying structure.

One of the key criteria for determining the blast resistance of the panels is their residual capacity, which we assessed through residual flexural strength after the blast tests. As a result of the blast loading, two out of the three bare panels tested retained residual strength, which was further evaluated using the four-point bending test. The third panel, however, experienced complete failure, as depicted in Figures 12 and 13. A lateral crack emerged at the centre of the panel, spanning the full width and a significant portion of the thickness of the cross-section, leaving only a few fibres connecting the two halves. Given its inability to support its own weight, we assumed

a residual strength of zero for this panel. This response might be potentially attributed to manufacturing parameters in the fracture region, possibly due to the arrangement and orientation of fibres in the panel’s critical cross-section, which compromised its flexural strength.

In contrast, the HPFRC panels with PU coating consistently exhibited residual strength. However, in one case, the residual strength was so negligible that the panel broke by hand during handling, rendering it ineligible for the four-point bending test. Therefore, we consider it reasonable to assume that the residual strength of this panel is insignificantly small.

This means that four out of six panels were available for the four-point bending test, comprising two coated and two bare panels. Additionally, three reference samples underwent the four-point bending test to establish the properties of undamaged HPFRC panels for comparison. The average maximum loading force for undamaged panels, as well as the maximum loading force for each of the blast-tested panels, is provided in Table 5. These results are further illus-

Sample	Loading force [kN]	Flexural strength [MPa]	Absorbed energy up to 16 mm deflection [J]
REF	13.16	15.43	319.68
Bare	8.18 (−38 %)	9.59 (−38 %)	171.30 (−46 %)
	6.98 (−47 %)	8.18 (−47 %)	141.99 (−56 %)
Coated	3.71 (−72 %)	4.35 (−72 %)	63.38 (−80 %)
	5.97 (−55 %)	7.00 (−55 %)	125.74 (−61 %)

TABLE 5. Results of the four-point bending test.

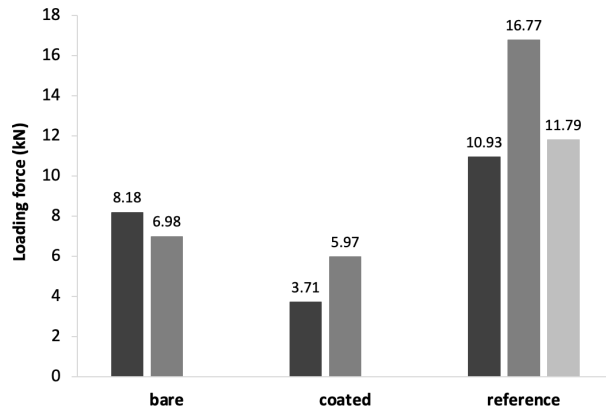


FIGURE 14. Comparison of maximum loading force in tested samples.

trated in the accompanying diagram in Figure 14. Furthermore, the relationship between the loading force and deflection for all samples during the four-point bending test is depicted in Figure 15. Due to the termination of measurements, the diagram shows a maximum deflection of 16 mm.

From the maximum loading force and the cross-section dimensions, the flexural strength of each panel is determined using the relation displayed in Equation (1) and presented in Table 5. A linear stress distribution is assumed for the calculation of the flexural strength (σ_{\max}):

$$\sigma_{\max} = \frac{M_{\max}}{W} = \frac{M_{\max}}{\frac{b \times h^2}{6}}, \quad (1)$$

where

M_{\max} is the maximum bending moment,

W is the section modulus,

b is the panel's width,

h is the panel's thickness.

The results are presented in Table 5 as well.

Our findings indicate that bare HPFRC panels, after blast testing, withstand between 50 % and 75 % of the loading force relative to undamaged panels. In contrast, HPFRC panels with PU coating exhibit less than 50 % flexural strength compared to undamaged panels. The explanation to these findings might be that while all bare HPFRC panels experienced localised complete perforation, the blast passed through

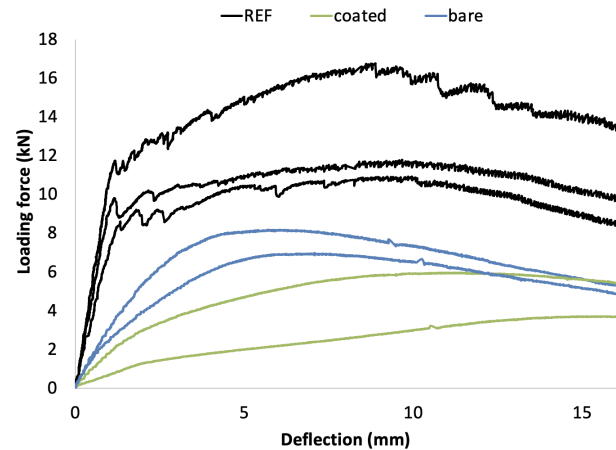


FIGURE 15. Four-point bending test deflection-loading force dependence.

the panel in a single crater without inducing much damage to the rest of the panel. Conversely, the PU coating prevented complete perforation by reflecting a portion of the wave back into the panel, thereby dissipating the blast energy throughout the panel and thus causing damage to a larger area. Coated panels absorbed more blast energy than uncoated ones, possibly explaining why they fail at lower loading forces. It seems the effectiveness of the PU coating lies primarily in preventing the complete perforation and fragmentation during a blast rather than enhancing the post-blast resistance of the panel.

The results of the four-point bending test can be juxtaposed with the results outlined in [2]. Notably, there are variations in the test setup, particularly in the distances between the supports and the hydraulic jack's contact points. Nonetheless, the average flexural strength of 15.43 MPa determined in this study for reference samples remains notably consistent with the findings of Mára et al. [2], who reported an average value of 14.4 MPa for undamaged panels.

It is also worth noting that the residual flexural strength of the bare panels damaged by the projectile impact was determined by Mára et al. [2] to be 11.2 MPa. The average residual flexural strength of bare panels damaged by a direct contact blast was found to be 8.9 MPa in this work. Since the projectile impact causes more concentrated damage, a higher residual bending strength can be expected.

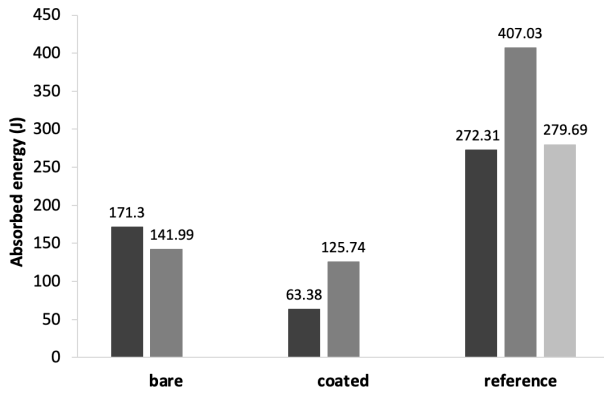


FIGURE 16. Comparison of absorbed energy of samples during four-point bending test.

To further compare samples, another parameter we considered is the absorbed energy of the panel during the four-point bending test, corresponding to the area below the loading force-deflection curve. For the comparison, we chose the absorbed energy up to a deflection of 16 mm, which we determined for each sample from the diagram displayed in Figure 15, using the relation as shown in:

$$E = \int_0^{16 \text{ mm}} f(x) dx. \quad (2)$$

The average absorbed energy up to 16 mm deflection for undamaged panels, together with the absorbed energy for each blast-tested panel is presented in Table 5. To provide a clearer representation, the absorbed energy for each sample is also shown in Figure 16. The findings reveal that uncoated panels previously subjected to blast absorb approximately half the energy absorbed by undamaged panels during the four-point bending test up to a 16 mm deflection. In contrast, coated panels absorb around 25 % of the energy compared to reference panels.

The blast experiments and subsequent testing and data assessment showed that the rear layer of PU coating effectively contained fragments in all instances, thereby mitigating the risk. However, our experiments did not conclusively establish whether the front PU layer enhances resistance. When designing the PU-coated HPFRC panels, our priority was simplicity and clarity in structure, especially for rapid assembly in short period of time. One of our main goals was to keep the possibility of a rapid construction of the protective barriers to which contributes the double-sided nature of the panels. This design feature facilitates swift, error-free construction of protective barriers by security personnel. Additionally, it proves beneficial in scenarios where the direction of danger is uncertain, offering equal protection from both sides. To comprehensively examine the impact of the front PU coating layer, future research will investigate HPFRC panels with single and double-sided PU coatings.

4. CONCLUSION

The main objective of our work was to evaluate the effectiveness of a polyurethane coating in enhancing the resistance of HPFRC protective panels to direct contact explosions. To investigate this, the area of the craters, cracking patterns, formation of rear fragments, post-test bending strength, and absorbed energy were closely examined. To the best of the authors' knowledge, the data presented in this study is the first of its kind and thus represents a novel contribution to the field. From the results of the study, several key inferences can be drawn:

- (1.) The application of a PU coating on both sides improves the blast resistance of HPFRC panels.
- (2.) For all tested samples without PU coating, complete perforation of the panel occurred during blast tests.
- (3.) For all tested samples, the application of PU coating prevented full perforation of the panel during blast tests.
- (4.) The PU coating on the back of the HPFRC panel was effective in holding back fragments during blast tests.
- (5.) A detailed scan revealed that the average crater area on the front surface for the coated samples is reduced by nearly 25 %, while the average crater area on the back surface is almost 23 % larger compared to the bare panels.
- (6.) In contrast to the bare panels, the PU-coated panels display a circular crack pattern, likely due to deformation inconsistencies between the front PU layer and the HPFRC panel.
- (7.) HPFRC panels with PU coating subjected to a blast test show less than 50 % of the bending strength of undamaged panels.
- (8.) Bare HPFRC panels subjected to blast testing show an increase in residual bending strength of up to 25 % compared to PU-coated panels.
- (9.) PU-coated panels showed increased energy absorption during blast, resulting in greater damage to the panel compared to bare samples.
- (10.) PU-coated panels showed a circumferential crack pattern on the front surface, which could be caused by deformation inconsistencies between the front PU layer and the HPFRC panel, similar to the observation of Hou et al. in [12].
- (11.) PU-coated panels absorbed, on average, 40 % less energy during the four-point bending test compared to bare panels.

ACKNOWLEDGEMENTS

This publication was supported by the Technology Agency of the Czech Republic (grant number FW03010141) and the Grant Agency of the CTU in Prague (grant number SGS24/051/OHK1/1T/11).

REFERENCES

- [1] J. Fornůšek, J. V., M. Mára, et al. Ballistic panel and ballistic system. US Patent US 10,648,780 B2, 2020.
- [2] M. Mára, C. Talone, R. Sovják, et al. Experimental investigation of thin-walled UHPFRCC modular barrier for blast and ballistic protection. *Applied Sciences* **10**(23):8716, 2020. <https://doi.org/10.3390/app10238716>
- [3] P. Hála, A. Perrot, B. Vacková, et al. Experimental and numerical study on ballistic resistance of polyurethane-coated thin HPFRC plate. *Materials Today: Proceedings* **93**:607–613, 2023. <https://doi.org/10.1016/j.matpr.2023.03.636>
- [4] P. Hála, P. Kheml, A. Perrot, et al. Lightweight protective sandwich structure with UHPC core. *International Interactive Symposium on Ultra-High Performance Concrete* **3**(1):16, 2023. <https://doi.org/10.21838/uhpc.16647>
- [5] P. Si, Y. Liu, J. Yan, et al. Effect of polyurea layer on ballistic behavior of ceramic/metal armor. *Structures* **48**:1856–1867, 2023. <https://doi.org/10.1016/j.istruc.2023.01.089>
- [6] Q. Liu, B. Guo, P. Chen, et al. Investigating ballistic resistance of CFRP/polyurea composite plates subjected to ballistic impact. *Thin-Walled Structures* **166**:108111, 2021. <https://doi.org/10.1016/j.tws.2021.108111>
- [7] P. Zhang, Z. Wang, P. Zhao, et al. Experimental investigation on ballistic resistance of polyurea coated steel plates subjected to fragment impact. *Thin-Walled Structures* **144**:106342, 2019. <https://doi.org/10.1016/j.tws.2019.106342>
- [8] S. A. Tekalur, A. Shukla, K. Shivakumar. Blast resistance of polyurea based layered composite materials. *Composite Structures* **84**(3):271–281, 2008. <https://doi.org/10.1016/j.compstruct.2007.08.008>
- [9] M. R. Amini, J. Isaacs, S. Nemat-Nasser. Investigation of effect of polyurea on response of steel plates to impulsive loads in direct pressure-pulse experiments. *Mechanics of Materials* **42**(6):628–639, 2010. <https://doi.org/10.1016/j.mechmat.2009.09.008>
- [10] M. R. Amini, J. Simon, S. Nemat-Nasser. Numerical modeling of effect of polyurea on response of steel plates to impulsive loads in direct pressure-pulse experiments. *Mechanics of Materials* **42**(6):615–627, 2010. <https://doi.org/10.1016/j.mechmat.2009.09.009>
- [11] M. R. Amini, J. B. Isaacs, S. Nemat-Nasser. Experimental investigation of response of monolithic and bilayer plates to impulsive loads. *International Journal of Impact Engineering* **37**(1):82–89, 2010. <https://doi.org/10.1016/j.ijimpeng.2009.04.002>
- [12] H. Hou, C. Chen, Y. Cheng, et al. Effect of structural configuration on air blast resistance of polyurea-coated composite steel plates: Experimental studies. *Materials & Design* **182**:108049, 2019. <https://doi.org/10.1016/j.matdes.2019.108049>
- [13] D. Mohotti, P. L. N. Fernando, D. Weerasinghe, A. Remennikov. Evaluation of effectiveness of polymer coatings in reducing blast-induced deformation of steel plates. *Defence Technology* **17**(6):1895–1904, 2021. <https://doi.org/10.1016/j.dt.2020.11.009>
- [14] S. Jia, C. Wang, W. Xu, et al. Experimental investigation on weak shock wave mitigation characteristics of flexible polyurethane foam and polyurea. *Defence Technology* **31**:179–191, 2024. <https://doi.org/10.1016/j.dt.2023.06.013>
- [15] J. LeBlanc, N. Gardner, A. Shukla. Effect of polyurea coatings on the response of curved E-Glass/Vinyl ester composite panels to underwater explosive loading. *Composites Part B: Engineering* **44**(1):565–574, 2013. <https://doi.org/10.1016/j.compositesb.2012.02.038>
- [16] Z. Bažantová, K. Kolář, P. Konvalinka, J. Litoš. Multi-functional high-performance cement based composite. *Key Engineering Materials* **677**:53–56, 2016. <https://doi.org/10.4028/www.scientific.net/KEM.677.53>
- [17] Z. Bažantová, K. Kolář, P. Konvalinka, et al. Controlled hardening of silicate binders for the optimization of high performance composites. *Key Engineering Materials* **722**:281–285, 2016. <https://doi.org/10.4028/www.scientific.net/KEM.722.281>
- [18] International Organization for Standardization. ISO 1183-1:2019. Plastics – Methods for determining the density of non-cellular plastics, 2019.
- [19] International Organization for Standardization. ISO 34-1:2022. Rubber, vulcanized or thermoplastic – Determination of tear strength, 2022. 5th edn.
- [20] ASTM. ASTM D1708-18. Standard test method for tensile properties of plastics by use of microtensile specimens, 2018. <https://doi.org/10.1520/D1708-18>